

BUDKERINP/2001-33
DFCAL-TH 01/2
June 2001

PHOTON-REGGEON INTERACTION VERTICES IN THE NLA *

V.S. Fadin^{a,b} †, D.Yu. Ivanov^{c,e} ‡ and M.I. Kotsky^{a,d} ††

^a *Budker Institute for Nuclear Physics, 630090 Novosibirsk, Russia*

^b *Novosibirsk State University, 630090 Novosibirsk, Russia*

^c *Institute of Mathematics, 630090 Novosibirsk, Russia*

^d *Istituto Nazionale di Fisica Nucleare, Gruppo collegato
di Cosenza, Arcavacata di Rende, I-87036 Cosenza, Italy*

^e *Regensburg University, Germany*

Abstract

We calculate the effective vertices for the quark-antiquark and the quark-antiquark-gluon production in the virtual photon - Reggeized gluon interaction. The last vertex is considered at the Born level; for the first one the one-loop corrections are obtained. These vertices have a number of applications; in particular, they are necessary for calculation of the virtual photon impact factor in the next-to-leading logarithmic approximation.

* *Work supported in part by INTAS and in part by the Russian Fund of Basic Researches.*

† *e-mail address:* FADIN@INP.NSK.SU

‡ *e-mail address:* D-IVANOV@MATH.NSC.RU

†† *e-mail address:* KOTSKY@INP.NSK.SU

1 Introduction

Investigation of processes with the Pomeron exchange remains to be one of the important problems of high energy physics. A special attention is attracted by the so called semi-hard processes, where large values of typical momentum transfers Q^2 give a possibility to use perturbative QCD for their theoretical description. The most common basis for such description is given by the BFKL approach [1]. It became widely known since discovery at HERA of the sharp rise of the proton structure function at decrease of the Bjorken variable x (see, for example, [2]). Recently the total cross section of the interaction of two highly virtual photons was measured at LEP. This process, being the one-scale process, seems to be even more natural for the application of the BFKL approach than the two-scale process of the deep inelastic scattering at small x , since here the evolution in x described by the BFKL equation does not interfere with the evolution in Q^2 described by the DGLAP equation.

For a consistent comparison with the experimental data the theoretical predictions must be obtained in the next-to-leading approximation (NLA), where together with the leading terms $(\alpha_s \ln(s))^n$ the terms $\alpha_s(\alpha_s \ln(s))^n$ are also resummed. The radiative corrections to the kernel of the BFKL equation were calculated several years ago [3]-[8] and the explicit form of the kernel of the equation in the NLA is known now [9, 10] for the case of forward scattering. But the problem of calculation in the NLA of the so called impact factors, which describe the coupling of the Pomeron to the scattering particles, remains unsolved.

Let us remind (see, for example, Ref. [11] for the details), that in the BFKL approach the relevant to the irreducible representation \mathcal{R} of the colour group in the t -channel part $(\mathcal{A}_{AB})_{A'B'}$ of the scattering amplitude for the process $AB \rightarrow A'B'$ at large c.m.s. energy $\sqrt{s} \rightarrow \infty$ and fixed momentum transfer $q \approx q_\perp$ (\perp means transverse to the initial particle momenta plane) is expressed in terms of the Mellin transform of the Green function of the two interacting Reggeized gluons $G_\omega^{(\mathcal{R})}$ and of the impact factors of the colliding particles $\Phi_{A'A}^{(\mathcal{R},\nu)}$ and $\Phi_{B'B}^{(\mathcal{R},\nu)}$:

$$\begin{aligned} \mathcal{I}m_s (\mathcal{A}_{AB})_{A'B'} &= \frac{s}{(2\pi)^{D-2}} \int \frac{d^{D-2}q_1}{\vec{q}_1^2(\vec{q}_1 - \vec{q})^2} \int \frac{d^{D-2}q_2}{\vec{q}_2^2(\vec{q}_2 - \vec{q})^2} \\ &\times \sum_\nu \Phi_{A'A}^{(\mathcal{R},\nu)}(\vec{q}_1, \vec{q}, s_0) \int_{\delta-i\infty}^{\delta+i\infty} \frac{d\omega}{2\pi i} \left[\left(\frac{s}{s_0} \right)^\omega G_\omega^{(\mathcal{R})}(\vec{q}_1, \vec{q}_2, \vec{q}) \right] \Phi_{B'B}^{(\mathcal{R},\nu)}(-\vec{q}_2, -\vec{q}, s_0), \end{aligned} \quad (1.1)$$

where $\mathcal{I}m_s$ means the s -channel imaginary part, the vector sign is used for denotation of the transverse components, ν enumerates the states in the representation \mathcal{R} , $D = 4 + 2\epsilon$ is the space-time dimension different from 4 to regularize both infrared and ultraviolet divergencies and the parameter s_0 is artificial and introduced for a convenience. While the Green function obeys the generalized BFKL equation [11]

$$\omega G_\omega^{(\mathcal{R})}(\vec{q}_1, \vec{q}_2, \vec{q}) = \vec{q}_1^2(\vec{q}_1 - \vec{q})^2 \delta^{(D-2)}(\vec{q}_1 - \vec{q}_2) + \int \frac{d^{D-2}k}{\vec{k}^2(\vec{k} - \vec{q})^2} \mathcal{K}^{(\mathcal{R})}(\vec{q}_1, \vec{k}, \vec{q}) G_\omega^{(\mathcal{R})}(\vec{k}, \vec{q}_2, \vec{q}) \quad (1.2)$$

with the NLA kernel $\mathcal{K}^{(\mathcal{R})}$ and is completely defined by this equation, the impact factors should be calculated separately. The definition of the NLA impact factors has been given in Ref. [11]; in the case of definite colours of c and c' of the Reggeized gluons the impact factor has a form [12]

$$\begin{aligned} \Phi_{AA'}^{cc'}(\vec{q}_1, \vec{q}, s_0) &= \left(\frac{s_0}{\vec{q}_1^2} \right)^{\frac{1}{2}\omega(-\vec{q}_1^2)} \left(\frac{s_0}{(\vec{q}_1 - \vec{q})^2} \right)^{\frac{1}{2}\omega(-(\vec{q}_1 - \vec{q})^2)} \\ &\times \sum_{\{f\}} \int \frac{d\kappa}{2\pi} \theta(s_\Lambda - \kappa) d\rho_f \Gamma_{\{f\}A}^c \left(\Gamma_{\{f\}A'}^{c'} \right)^* \\ &- \frac{1}{2} \int \frac{d^{D-2}k}{\vec{k}^2 (\vec{k} - \vec{q})^2} \Phi_{AA'}^{c_1 c'_1(Born)}(\vec{k}, \vec{q}, s_0) \left(\mathcal{K}_r^{Born} \right)_{c_1 c'}^{c'_1 c}(\vec{k}, \vec{q}_1, \vec{q}) \ln \left(\frac{s_\Lambda^2}{s_0 (\vec{k} - \vec{q}_1)^2} \right), \end{aligned} \quad (1.3)$$

where $\omega(t)$ is the Reggeized gluon trajectory and the intermediate parameter s_Λ should go to infinity. The integration in the first term of the above equality is carried out over the phase space $d\rho_f$ and over the squared invariant mass κ of the system $\{f\}$ produced in the fragmentation region of the particle A , $\Gamma_{\{f\}A}^c$ are the particle-Reggeon effective vertices for this production and the sum is taken over all systems $\{f\}$ which can be produced in the NLA. The second term in Eq. (1.3) is the counterterm for the LLA part of the first one, so that the logarithmic dependence of both terms on the intermediate parameter $s_\Lambda \rightarrow \infty$ disappears in their sum; \mathcal{K}_r^{Born} is the part of the leading order BFKL kernel related to the real gluon production (see Refs. [12] for more details). It was shown in Ref. [13] that the definition (1.3) guarantees infrared finiteness of the colourless particle impact factors.

It is clear from above that for complete NLA description in the BFKL approach one needs to know the impact factors, analogously as in the DGLAP approach one should know not only the parton distributions, but also the coefficient functions.

This paper is an extended version of the short note [14], which can be considered as the first step in the calculation of the virtual photon impact factor in the NLA. We calculate here the virtual photon-Reggeon effective vertices which enter the definition (1.3) in the case when the particle A is the virtual photon. In the NLA the states which can be produced in the Reggeon-virtual photon collision are the quark-antiquark and the quark-antiquark-gluon ones. In the next Section we present the effective vertices for production of these states in the Born approximation. This approximation is sufficient to find in the NLA the contribution to the virtual photon impact factor from the quark-antiquark-gluon state. In the case of the quark-antiquark state we need to know the effective production vertex with the one-loop accuracy. Sections 3-5 are devoted to the calculation of the one-loop corrections. In Sections 3 and 4 we consider the two-gluon and the one-gluon exchange diagrams correspondingly; in Section 5 the total one-loop correction is presented. The results obtained are discussed in Section 6. Some details of the calculation are given in Appendix A.

In the following the photon-Reggeon effective vertices presented in this paper will be used for the calculation of the photon impact factor. But they could have many other applications, for example, in the diffractive production of quark jets and so on.

2 The Born interaction vertices

In this section we present the vertices for the $q\bar{q}$ and the $q\bar{q}g$ production in the Reggeon-virtual photon collision in the Born approximation for the case of completely massless QCD. These vertices can be obtained from the high energy amplitudes with the octet colour state and the negative signature in the t -channel for collision of the virtual photon with any particle, if the corresponding system is produced in the virtual photon fragmentation region. For simplicity we always consider collision of the virtual photon with the momentum p_A and the quark with the momentum p_B . We use everywhere below the Feynman gauge for the gluon field, the Sudakov decomposition of momenta

$$p = \beta p_1 + \alpha p_2 + p_\perp, \quad \alpha = \frac{p^2 + \vec{p}_\perp^2}{s\beta}, \quad p_1^2 = p_2^2 = 0, \\ s = 2p_1 p_2 \rightarrow \infty, \quad \vec{p}_\perp^2 \equiv -p_\perp^2, \quad (2.1)$$

with the lightcone basis in the longitudinal space defined by

$$p_A = p_1 - \frac{Q^2}{s} p_2, \quad p_A^2 = -Q^2, \quad p_B = p_2, \quad p_B^2 = 0, \quad (2.2)$$

and the usual trick of retaining only the first term in the decomposition of the metric tensor

$$g^{\mu\nu} = \frac{2p_2^\mu p_1^\nu}{s} + \frac{2p_1^\mu p_2^\nu}{s} + g_\perp^{\mu\nu} \rightarrow \frac{2p_2^\mu p_1^\nu}{s} \quad (2.3)$$

in the numerator of the gluon propagator connecting vertices μ and ν with momenta predominantly along p_1 and p_2 respectively. The virtual photon polarization vector e is taken in the gauge $ep_2=0$, so that

$$e = e_\perp + \frac{2ep_1}{s} p_2. \quad (2.4)$$

Then the polarization vector \tilde{e} in the usual gauge $\tilde{e}p_A = 0$ is

$$\tilde{e} = e + \frac{ep_1}{Q^2} p_A, \quad (2.5)$$

so that in the case of the longitudinal polarization, when $\tilde{e}_L^2 = 1$, we have $e_L p_1 = Q$.

Let us start with the calculation of the quark-antiquark production vertex. The diagrams of the production process contributing in the Regge asymptotics are shown in Fig. 1.

As was already mentioned, the quark-antiquark pair is produced in the photon fragmentation region, so that the invariant mass $\sqrt{\kappa}$ of the pair is of order of typical transverse momenta and doesn't grow with s . The Regge form of the production amplitude $\mathcal{A}_{Q\gamma^* \rightarrow Qq\bar{q}}^{(0)}$ is

$$\mathcal{A}_{Q\gamma^* \rightarrow Qq\bar{q}}^{(0)} = \Gamma_{\gamma^* q\bar{q}}^{c(0)} \frac{2s}{t} \Gamma_{QQ}^{c(0)}, \quad (2.6)$$

where $t = q^2$ and $\Gamma_{\gamma^* q\bar{q}}^{c(0)}$ and $\Gamma_{QQ}^{c(0)}$ are corresponding particle-Reggeon effective vertices in the Born approximation. Let us note, that the amplitude of Fig. 1 has automatically

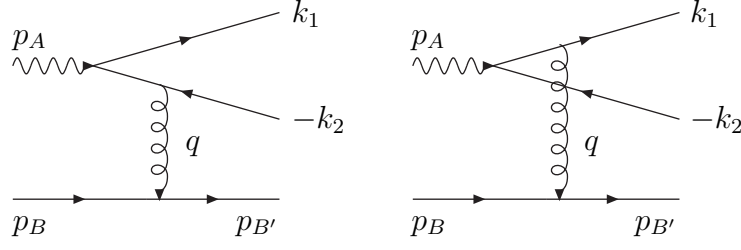


Figure 1: The lowest order Feynman diagrams for the process $\gamma^* Q \rightarrow (q\bar{q})Q$.

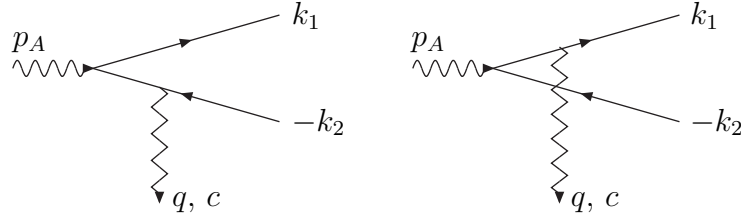


Figure 2: Schematic representation of the vertex $\Gamma_{\gamma^* q\bar{q}}^{c(0)}$.

only the octet colour state and the negative signature in the t -channel, so that it is not necessary here to perform any projection. The notations for all momenta are shown in Fig. 1. The quark-Reggeon vertex is known up to the NLA accuracy and its Born part is

$$\Gamma_{QQ}^{c(0)} = gt_{B'B}^c \bar{u}_{B'} \frac{\not{p}_1}{s} u_B, \quad (2.7)$$

where g is the coupling constant, t^c are the colour group generators in the fundamental representation and u is a quark spinor wave function. Then, comparing Eqs. (2.6), (2.7) with the explicit form of the amplitude given by the diagrams of Fig. 1, one can easily obtain for $\Gamma_{\gamma^* q\bar{q}}^{c(0)}$ the diagrammatic representation of Fig. 2 (see Ref. [13]), where the zig-zag lines represent the Reggeon with the momentum

$$q = -\frac{\kappa + Q^2 + \vec{q}^2}{s} p_2 + q_\perp, \quad t = q^2 = q_\perp^2 = -\vec{q}^2, \quad (2.8)$$

and the colour index c . The lowest order effective vertices for interaction of the Reggeon with quarks and gluons are defined in Fig. 3 (see Ref. [13]).

The vertex $\Gamma_{\gamma^* q\bar{q}}^{c(0)}$ can be obtained from the diagrams of Fig. 2 by the usual Feynman rules as the amplitude of the quark-antiquark production in collision of the virtual photon with the Reggeon. This procedure gives us the result

$$\Gamma_{\gamma^* q\bar{q}}^{c(0)} = -eq_f gt_{i_1 i_2}^c \bar{u}_1 \left(\frac{\hat{\Gamma}_1}{t_1} - \frac{\hat{\Gamma}_2}{t_2} \right) \frac{\not{p}_2}{s} v_2 = -eq_f gt_{i_1 i_2}^c \left(\left[\bar{u}_1 \frac{\hat{\Gamma}_1}{t_1} \frac{\not{p}_2}{s} v_2 \right] - [1 \leftrightarrow 2] \right), \quad (2.9)$$

where eq_f is the electric charge of the produced quark, i_1 and i_2 are the colour indices of the quark and antiquark correspondingly, v is the spinor wave function of the produced

(a)
(b)

Figure 3: The quark-quark-Reggeon and the gluon-gluon-Reggeon effective vertices. T^c is the colour group generator in the adjoint representation.

antiquark,

$$\hat{\Gamma}_1 = \frac{1}{x_1} (2x_2(ek_1) - \not{\epsilon}_\perp \not{k}_{1\perp}), \quad \hat{\Gamma}_2 = \frac{1}{x_2} (2x_1(ek_2) - \not{k}_{2\perp} \not{\epsilon}_\perp),$$

$$t_i = (p_A - k_i)^2 = -\frac{\vec{k}_i^2 + x_1 x_2 Q^2}{x_i}, \quad (2.10)$$

with the variables x_i defined by the Sudakov decompositions of the produced quark and antiquark momenta

$$k_i = x_i p_1 + \frac{\vec{k}_i^2}{s x_i} p_2 + k_{i\perp}, \quad k_i^2 = 0, \quad i = 1, 2. \quad (2.11)$$

The substitution $1 \leftrightarrow 2$ in Eq. (2.9) means replacement quark \leftrightarrow antiquark, i.e. $x_1 \leftrightarrow x_2$, $\vec{k}_1 \leftrightarrow \vec{k}_2$ together with replacement of the polarizations. Validity of the second equality in (2.9) can be easily verified using the charge conjugation matrix. We will need later the Born effective vertex $\Gamma_{\gamma^* q\bar{q}}^{c(0)}$ also in the helicity representation for the case of the space-time dimension D equal 4. To obtain it we use the polarization matrix

$$\hat{\rho} \equiv (v_2 \bar{u}_1) = \frac{1}{\sqrt{x_1 x_2}} \frac{1}{4} \left[\left(x_2 k_1 + x_1 k_2 - \kappa \frac{p_2}{s} \right)^\mu - 2i\xi e^{\mu\nu\sigma\rho} k_{2\nu} k_{1\sigma} \frac{p_{2\rho}}{s} \right] \gamma_\mu (1 - \xi \gamma_5), \quad (2.12)$$

where

$$e^{0123} = 1, \quad \gamma_5 = i\gamma^0 \gamma^1 \gamma^2 \gamma^3, \quad (2.13)$$

and $\xi = \pm 1$ is a double helicity of the produced quark. The polarization matrix satisfies the evident relations

$$\not{k}_2 \hat{\rho} = \hat{\rho} \not{k}_1 = (1 - \xi \gamma_5) \hat{\rho} = \hat{\rho} (1 + \xi \gamma_5) = 0. \quad (2.14)$$

For the virtual photon polarization vector we also use the helicity representation

$$e^\mu(\lambda) = \frac{1}{\sqrt{-2t}} \left[(\delta_{\lambda,1} + \delta_{\lambda,-1}) \left(q_\perp^\mu + 2i\lambda e^{\mu\nu\sigma\rho} q_\nu p_{1\sigma} \frac{p_{2\rho}}{s} \right) + \delta_{\lambda,0} \sqrt{-2t} Q^2 \frac{2p_2^\mu}{s} \right], \quad \lambda = 0, \pm 1. \quad (2.15)$$

Using Eqs. (2.9) - (2.15) we get

$$\Gamma_{\gamma^* q\bar{q}}^{c(0)} = -\frac{2eq_f g t_{i_1 i_2}^c}{\sqrt{-2t x_1 x_2}} \left(\left[\frac{x_2}{t_1} \{ \delta_{\lambda,0} \sqrt{2} q Q x_1 x_2 - \right. \right.$$

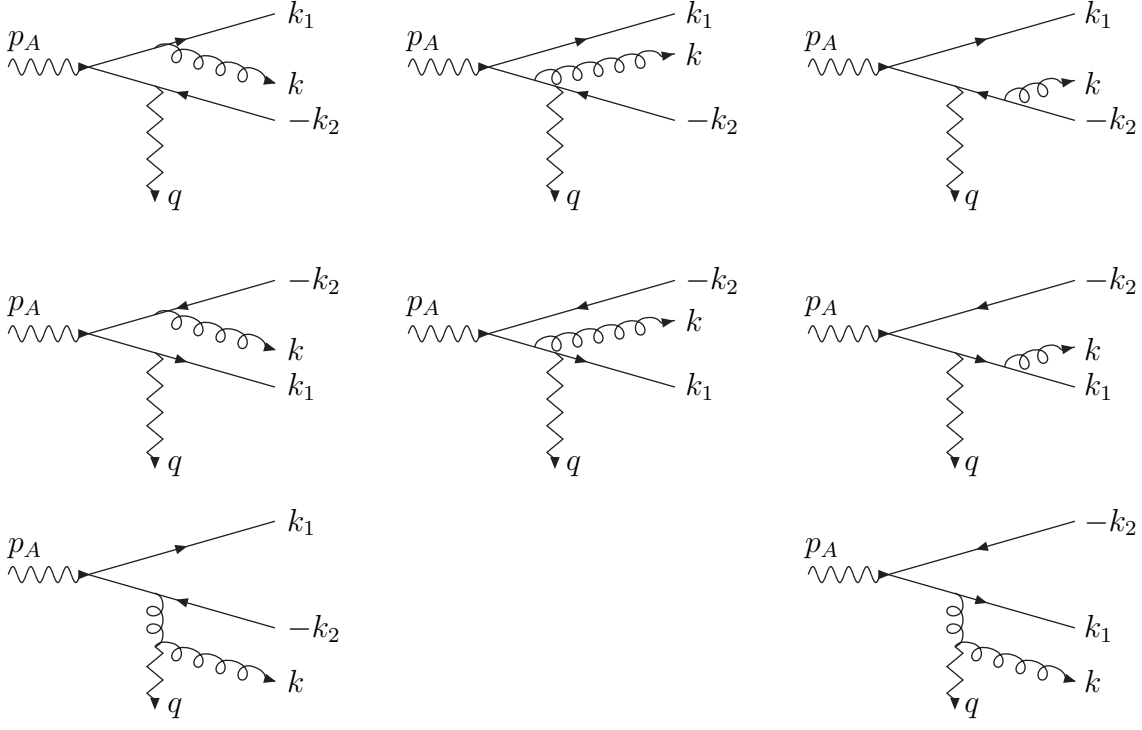


Figure 4: Schematic representation of the vertex $\Gamma_{\gamma^* q \bar{q} g}^{c(0)}$.

$$\begin{aligned}
& -(\vec{k}_1 \vec{q} + i\lambda P) (x_2 \delta_{\lambda, -\xi} - x_1 \delta_{\lambda, \xi}) \Big] - [1 \leftrightarrow 2] \Big) = \\
& = \frac{2eq_f g t_{i_1 i_2}^c}{\sqrt{-2tx_1 x_2}} \left[\delta_{\lambda, 0} \sqrt{2} q Q x_1 x_2 \left(\frac{x_1}{t_2} - \frac{x_2}{t_1} \right) \right. \\
& \left. + (x_2 \delta_{\lambda, -\xi} - x_1 \delta_{\lambda, \xi}) \left(\frac{x_2}{t_1} (\vec{k}_1 \vec{q} + i\lambda P) + \frac{x_1}{t_2} (\vec{k}_2 \vec{q} - i\lambda P) \right) \right], \quad (2.16)
\end{aligned}$$

where $q = |\vec{q}|$,

$$P = 2e^{\mu\nu\sigma\rho} k_{1\mu} k_{2\nu} p_{1\sigma} \frac{p_{2\rho}}{s}, \quad (2.17)$$

with the property $P^2 = \vec{k}_1^2 \vec{k}_2^2 - (\vec{k}_1 \vec{k}_2)^2$, and the replacement $(1 \leftrightarrow 2)$ is $x_1 \leftrightarrow x_2$, $\vec{k}_1 \leftrightarrow \vec{k}_2$, $\xi \leftrightarrow -\xi$.

Next we do is the calculation of the quark-antiquark-gluon production effective vertex $\Gamma_{\gamma^* q \bar{q} g}^{c(0)}$. It can be obtained through the usual Feynman rules with the elementary Reggeon vertices defined at Fig. 3 as the amplitude of the quark-antiquark-gluon production in the virtual photon-Reggeon collision represented by the diagrams of Fig. 4, where the denotations of momenta are presented. The colour indices of the Reggeon and the emitted gluon are c and b respectively. The Reggeon momentum is given by Eq. (2.8), where κ now is the quark-antiquark-gluon squared invariant mass. The vertex $\Gamma_{\gamma^* q \bar{q} g}^{c(0)}$ obtained in this way is invariant with respect to the gauge transformations of the emitted gluon polarization vector e_g and can be simplified by appropriate choice of the gauge. We use the axial gauge

$$e_g p_2 = 0, \quad e_g = -\frac{2(e_{g\perp} k_\perp)}{s\beta} p_2 + e_{g\perp}, \quad (2.18)$$

where β is defined by $k = \beta p_1 + \vec{k}_\perp^2 / (s\beta) p_2 + k_\perp$. In this gauge the last nonlocal term in the expression for the gluon-Reggeon interaction vertex of Fig. 3(b) disappears and we

obtain

$$\begin{aligned}
\Gamma_{\gamma^* q \bar{q} g}^{c(0)} (e q_f g^2)^{-1} &= \langle 1 | t^b t^c | 2 \rangle \left[\bar{u}_1 \left\{ \frac{1}{(p_A - k_1)^2 (k_2 + q)^2} \not{\epsilon}(\not{p}_A - \not{k}_1) \not{\epsilon}_g^*(\not{k}_2 + \not{q}) \frac{\not{p}_2}{s} \right. \right. \\
&+ \frac{1}{(k + k_1)^2 (p_A - k_2)^2} \not{\epsilon}_g^*(\not{k} + \not{k}_1) \frac{\not{p}_2}{s} (\not{p}_A - \not{k}_2) \not{\epsilon} - \frac{1}{(k + k_1)^2 (k_2 + q)^2} \not{\epsilon}_g^*(\not{k} + \not{k}_1) \not{\epsilon} \times \\
&\times (\not{k}_2 + \not{q}) \frac{\not{p}_2}{s} + \left. \left(\frac{\gamma_\mu (\not{p}_A - \not{k}_2) \not{\epsilon}}{(p_A - k_2)^2} - \frac{\not{\epsilon} (\not{p}_A - \not{k}_1) \gamma_\mu}{(p_A - k_1)^2} \right) \frac{1}{(k + q)^2} \left(\beta e_g^{*\mu} - \frac{p_2^\mu}{s} (2q e_g^*) \right) \right\} v_2 \Big] \\
&+ \langle 1 | t^c t^b | 2 \rangle [1 \leftrightarrow 2] = \\
&= \langle 1 | t^b t^c | 2 \rangle \left[\bar{u}_1 \left\{ \frac{1}{(p_A - k_1)^2 (k_2 + q)^2} \not{\epsilon}(\not{p}_A - \not{k}_1) \not{\epsilon}_g^*(\not{k}_2 + \not{q}) \frac{\not{p}_2}{s} + \frac{1}{(k + k_1)^2 (p_A - k_2)^2} \times \right. \right. \\
&\times \not{\epsilon}_g^*(\not{k} + \not{k}_1) \frac{\not{p}_2}{s} (\not{p}_A - \not{k}_2) \not{\epsilon} - \frac{1}{(k + k_1)^2 (k_2 + q)^2} \not{\epsilon}_g^*(\not{k} + \not{k}_1) \not{\epsilon} (\not{k}_2 + \not{q}) \frac{\not{p}_2}{s} \\
&+ \left. \left(\frac{\gamma_\mu (\not{p}_A - \not{k}_2) \not{\epsilon}}{(p_A - k_2)^2} - \frac{\not{\epsilon} (\not{p}_A - \not{k}_1) \gamma_\mu}{(p_A - k_1)^2} \right) \frac{1}{(k + q)^2} \left(\beta e_g^{*\mu} - \frac{p_2^\mu}{s} (2q e_g^*) \right) \right\} v_2 \Big] \\
&+ \langle 1 | t^c t^b | 2 \rangle \left[\bar{u}_1 \left\{ \frac{1}{(p_A - k_2)^2 (k_1 + q)^2} \frac{\not{p}_2}{s} (\not{k}_1 + \not{q}) \not{\epsilon}_g^*(\not{p}_A - \not{k}_2) \not{\epsilon} + \frac{1}{(k + k_2)^2 (p_A - k_1)^2} \times \right. \right. \\
&\times \not{\epsilon}(\not{p}_A - \not{k}_1) \frac{\not{p}_2}{s} (\not{k} + \not{k}_2) \not{\epsilon}_g^* - \frac{1}{(k + k_2)^2 (k_1 + q)^2} \frac{\not{p}_2}{s} (\not{k}_1 + \not{q}) \not{\epsilon} (\not{k} + \not{k}_2) \not{\epsilon}_g^* \\
&+ \left. \left(\frac{\not{\epsilon} (\not{p}_A - \not{k}_1) \gamma_\mu}{(p_A - k_1)^2} - \frac{\gamma_\mu (\not{p}_A - \not{k}_2) \not{\epsilon}}{(p_A - k_2)^2} \right) \frac{1}{(k + q)^2} \left(\beta e_g^{*\mu} - \frac{p_2^\mu}{s} (2q e_g^*) \right) \right\} v_2 \Big]. \quad (2.19)
\end{aligned}$$

3 The one-loop correction: the two-gluon exchange diagrams

In this section we consider the contribution of the two gluon exchange diagrams to $\Gamma_{\gamma^* q \bar{q}}^c$. There are six diagrams of such kind for the process we consider; they are shown at Fig. 5.

Now we have to perform the projection on the negative signature and the octet colour state in the t -channel. It is done by the following replacement of the colour factor of the lowest line of the diagrams Fig. 5:

$$(t^b t^a)_{B'B} \rightarrow \frac{1}{2} (t^b t^a - t^a t^b)_{B'B} = \frac{1}{2} T_{ab}^c t_{B'B}^c. \quad (3.1)$$

Then we obtain

$$\mathcal{A}_{Q\gamma^* \rightarrow Qq\bar{q}}^{(2g)(8,-)(1)} = \frac{1}{4} N t_{i_1 i_2}^c t_{B'B}^c \{ [(D_1 + D_2) - (1 \leftrightarrow 2)] - [s \leftrightarrow -s] \}, \quad (3.2)$$

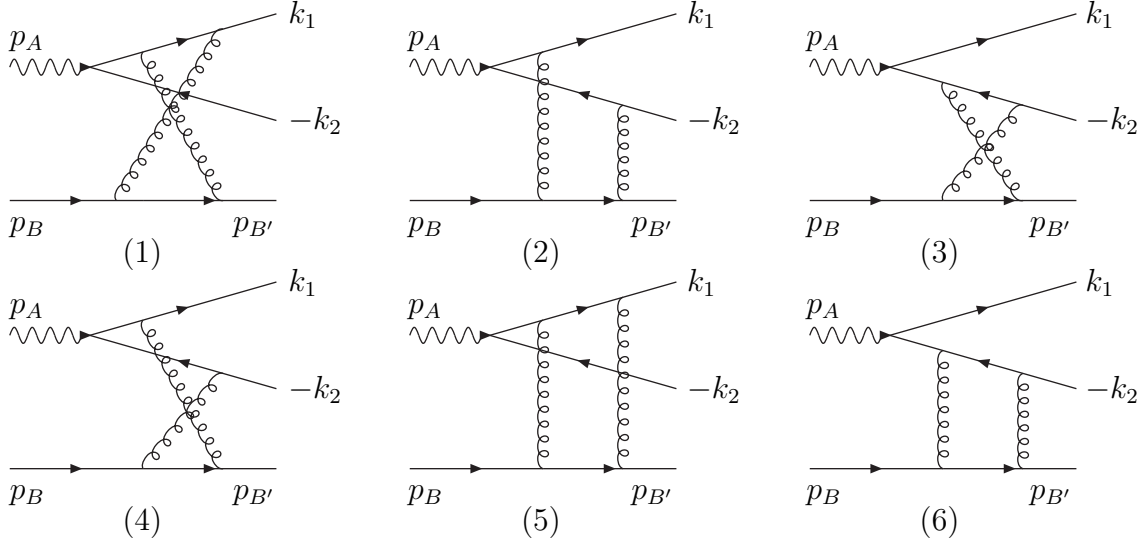


Figure 5: The two-gluon exchange Feynman diagrams for the process $\gamma^*Q \rightarrow (q\bar{q})Q$.

where N is the number of colours, D_1 is the amplitude represented by the diagram of Fig. 5(1) with omitted colour generators in any its vertex, and $2D_2$ is such amplitude for the diagram of Fig. 5(2).

The calculation of D_1 is quite straightforward. Note here that since our final goal is the virtual photon impact factor in the physical space-time, and since the integration over the quark-antiquark states in Eq. (1.3) is not singular, we need to retain in the vertex $\Gamma_{\gamma^*q\bar{q}}^c$ and consequently in the amplitude $\mathcal{A}_{Q\gamma^*\rightarrow Qq\bar{q}}^{(2g)(8,-)^{(1)}}$ only the terms which do not vanish at $\epsilon \rightarrow 0$. Therefore all one-loop results are presented in this paper with such accuracy. In the convenient for us form we have

$$\begin{aligned}
(D_1 - D_1(1 \leftrightarrow 2)) - (s \leftrightarrow -s) &= \frac{4}{N} g \bar{u}_{B'} \frac{\not{p}_1}{s} u_B(-) e q_f g \bar{u}_1 \left(\frac{\hat{\Gamma}_1}{t_1} - \frac{\hat{\Gamma}_2}{t_2} \right) \frac{\not{p}_2}{s} v_2 \frac{s}{t} \omega^{(1)}(t) \\
&\times \left(\ln \left(\frac{s}{-t} \right) + \ln \left(\frac{-s}{-t} \right) \right) + 4g \bar{u}_{B'} \frac{\not{p}_1}{s} u_B \frac{2s}{t} e q_f g^3 \frac{\Gamma(2-\epsilon)}{(4\pi)^{2+\epsilon}} \frac{1}{2\epsilon} \\
&\times \left\{ \left[\bar{u}_1 \frac{\hat{\Gamma}_1}{t_1} \frac{\not{p}_2}{s} v_2 \left(2(-t)^\epsilon \left(\frac{1}{\epsilon} + 1 + 2(1+\epsilon) \ln x_2 + \epsilon - 5\epsilon\psi'(1) \right) \right) \right. \right. \\
&\left. \left. + \int_0^1 \frac{dy}{(-(1-y)t - yt_1)^{1-\epsilon}} 2(1+\epsilon) (t - 2(t-t_1)y^\epsilon) \right] - [1 \leftrightarrow 2] \right\}, \quad (3.3)
\end{aligned}$$

where the first term is responsible for the Reggeization of the amplitude $\mathcal{A}_{Q\gamma^*\rightarrow Qq\bar{q}}^{(8,-)}$ with $\omega^{(1)}$ being the one-loop Reggeized gluon trajectory,

$$\omega^{(1)}(t) = -g^2 N \frac{\Gamma(1-\epsilon)}{(4\pi)^{2+\epsilon}} (\vec{q}^2)^\epsilon \frac{\Gamma^2(\epsilon)}{\Gamma(2\epsilon)}, \quad (3.4)$$

and $\Gamma(z)$ and $\psi(z)$ are the Euler Γ -function and its logarithmic derivative correspondingly. The calculation of D_2 is more complicated and we present some details of it in the Appendix. Here we write down only the result

$$(D_2 - D_2(1 \leftrightarrow 2)) - (s \leftrightarrow -s) = 4g \bar{u}_{B'} \frac{\not{p}_1}{s} u_B \frac{2s}{t} e q_f g^3 \frac{\Gamma(2-\epsilon)}{(4\pi)^{2+\epsilon}} \frac{1}{2\epsilon}$$

$$\begin{aligned}
& \times \left\{ \left[\bar{u}_1 \int_0^1 \int_0^1 \frac{dy_1 dy_2}{[(1-y_2)(-(1-y_1)t - y_1 t_2) + y_2(-(1-y_1)t_1 + y_1 Q^2)]^{2-\epsilon}} \left(y_1^{\epsilon-1} (1-y_1) y_2^{-\epsilon} \right. \right. \right. \\
& \quad \times \left(x_1^\epsilon x_2^{-\epsilon} - 2\epsilon^2 \psi'(1) \right) 2t \hat{\Gamma}_1 + (1-y_1) 4t (ek_1) \\
& \quad \left. \left. \left. + \left(y_1^\epsilon y_2^{-\epsilon} x_1^\epsilon x_2^{-\epsilon} - 1 \right) 4x_2 t (ep_1) \right) \frac{\not{p}_2}{s} v_2 \right] - [1 \leftrightarrow 2] \right\}. \tag{3.5}
\end{aligned}$$

Note that the imaginary parts of D_2 (in the $(p_{B'} + k_2)^2$ -channel) and $D_2(1 \leftrightarrow 2)$ (in the $(p_{B'} + k_1)^2$ -channel) which would destroy the Reggeization cancel in the amplitude $\mathcal{A}_{Q\gamma^* \rightarrow Qq\bar{q}}^{(8,-)}$. Although in the NLA BFKL approach there is no requirement of the Reggeization of full amplitudes (the Reggeization of their real parts is sufficient), we see that nevertheless the Reggeization holds also without omitting of any imaginary part for the process $Q\gamma^* \rightarrow Qq\bar{q}$.

The amplitude $\mathcal{A}_{Q\gamma^* \rightarrow Qq\bar{q}}$ with the octet colour state and the negative signature in the t -channel has the following Reggeized form

$$\begin{aligned}
\mathcal{A}_{Q\gamma^* \rightarrow Qq\bar{q}}^{(8,-)} &= \Gamma_{\gamma^* q\bar{q}}^c \frac{s}{t} \left[\left(\frac{s}{-t} \right)^{\omega(t)} + \left(\frac{-s}{-t} \right)^{\omega(t)} \right] \Gamma_{QQ}^c \approx \Gamma_{\gamma^* q\bar{q}}^{c(0)} \frac{2s}{t} \Gamma_{QQ}^{c(0)} + \Gamma_{\gamma^* q\bar{q}}^{c(0)} \frac{s}{t} \omega^{(1)}(t) \\
& \times \left[\ln \left(\frac{s}{-t} \right) + \ln \left(\frac{-s}{-t} \right) \right] \Gamma_{QQ}^{c(0)} + \Gamma_{\gamma^* q\bar{q}}^{c(0)} \frac{2s}{t} \Gamma_{QQ}^{c(1)} + \Gamma_{\gamma^* q\bar{q}}^{c(1)} \frac{2s}{t} \Gamma_{QQ}^{c(0)}. \tag{3.6}
\end{aligned}$$

Let us now split the one-loop contributions to this amplitude and both of the effective vertices according to the three sets of the one-loop diagrams for $\mathcal{A}_{Q\gamma^* \rightarrow Qq\bar{q}}$: the two-gluon exchange diagrams, the t -channel gluon self-energy diagrams and the one-gluon exchange diagrams

$$\begin{aligned}
\mathcal{A}_{Q\gamma^* \rightarrow Qq\bar{q}}^{(2g)(8,-)(1)} + \mathcal{A}_{Q\gamma^* \rightarrow Qq\bar{q}}^{(se)(8,-)(1)} + \mathcal{A}_{Q\gamma^* \rightarrow Qq\bar{q}}^{(1g)(8,-)(1)} &= \left\{ \Gamma_{\gamma^* q\bar{q}}^{(2g)c(1)} \frac{2s}{t} \Gamma_{QQ}^{c(0)} + \Gamma_{\gamma^* q\bar{q}}^{c(0)} \frac{2s}{t} \Gamma_{QQ}^{(2g)c(1)} \right. \\
& \left. + \Gamma_{\gamma^* q\bar{q}}^{c(0)} \frac{s}{t} \omega^{(1)}(t) \left[\ln \left(\frac{s}{-t} \right) + \ln \left(\frac{-s}{-t} \right) \right] \Gamma_{QQ}^{c(0)} \right\} \\
& + \left\{ \Gamma_{\gamma^* q\bar{q}}^{(se)c(1)} \frac{2s}{t} \Gamma_{QQ}^{c(0)} + \Gamma_{\gamma^* q\bar{q}}^{c(0)} \frac{2s}{t} \Gamma_{QQ}^{(se)c(1)} \right\} + \left\{ \Gamma_{\gamma^* q\bar{q}}^{(1g)c(1)} \frac{2s}{t} \Gamma_{QQ}^{c(0)} + \Gamma_{\gamma^* q\bar{q}}^{c(0)} \frac{2s}{t} \Gamma_{QQ}^{(1g)c(1)} \right\}, \tag{3.7}
\end{aligned}$$

where the self-energy diagrams and one-gluon exchange diagrams have automatically only the octet colour state and negative signature in the t -channel, so that

$$\mathcal{A}_{Q\gamma^* \rightarrow Qq\bar{q}}^{(se)(8,-)(1)} \equiv \mathcal{A}_{Q\gamma^* \rightarrow Qq\bar{q}}^{(se)(1)}, \quad \mathcal{A}_{Q\gamma^* \rightarrow Qq\bar{q}}^{(1g)(8,-)(1)} \equiv \mathcal{A}_{Q\gamma^* \rightarrow Qq\bar{q}}^{(1g)(1)}. \tag{3.8}$$

We remind that in our case of completely massless quantum field theory the contribution from the renormalization of the external lines is absent in the dimensional regularization. Now, from the representations of Eqs. (3.7), (3.8) it is easy to see that $\Gamma_{\gamma^* q\bar{q}}^{(1g)c(1)}$ is given by the radiative corrections to the amplitude of the quark-antiquark production in collision of the virtual photon with the gluon having momentum q , colour index c and polarization vector $-p_2^\mu/s$, whereas $\Gamma_{QQ}^{(1g)c(1)}$ is defined by the radiative corrections to the vertex of interaction of this gluon with the quark Q . In both cases the gluon self-energy is not

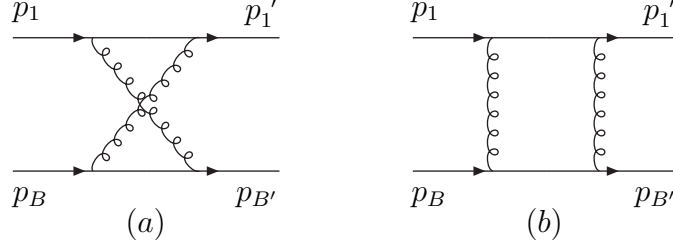


Figure 6: The two-gluon exchange Feynman diagrams for the process $qQ \rightarrow qQ$.

included into these corrections; it is divided in equal parts between $\Gamma_{\gamma^* q\bar{q}}^{(se)c(1)}$ and $\Gamma_{QQ}^{(se)c(1)}$. For the two-gluon exchange contributions we have the relation:

$$\Gamma_{\gamma^* q\bar{q}}^{(2g)c(1)} \frac{2s}{t} \Gamma_{QQ}^{c(0)} + \Gamma_{\gamma^* q\bar{q}}^{c(0)} \frac{2s}{t} \Gamma_{QQ}^{(2g)c(1)} = \mathcal{A}_{Q\gamma^* \rightarrow Qq\bar{q}}^{(2g)(8,-)(1)} - \Gamma_{\gamma^* q\bar{q}}^{c(0)} \frac{s}{t} \omega^{(1)}(t) \left[\ln\left(\frac{s}{-t}\right) + \ln\left(\frac{-s}{-t}\right) \right] \Gamma_{QQ}^{c(0)}, \quad (3.9)$$

which shows that we need to know the correction $\Gamma_{QQ}^{(2g)c(1)}$. This correction can be obtained from the two-gluon contribution to the Qq elastic scattering amplitude with the colour octet and the negative signature in the t -channel in the Regge kinematical region. From Eq. (3.9) with the replacements

$$\Gamma_{\gamma^* q\bar{q}}^{(2g)c(0,1)} \rightarrow \Gamma_{qq}^{(2g)c(0,1)}, \quad \mathcal{A}_{Q\gamma^* \rightarrow Qq\bar{q}}^{(2g)(8,-)(1)} \rightarrow \mathcal{A}_{Qq \rightarrow Qq}^{(2g)(8,-)(1)}, \quad (3.10)$$

denoting

$$\Gamma_{qq}^{(2g)c(1)} = \delta^{(2g)}(t) \Gamma_{qq}^{c(0)}, \quad \Gamma_{QQ}^{(2g)c(1)} = \delta^{(2g)}(t) \Gamma_{QQ}^{c(0)} \quad (3.11)$$

we get

$$\delta^{(2g)}(t) = \frac{t}{4s \Gamma_{qq}^{c(0)} \Gamma_{QQ}^{c(0)}} \left\{ \mathcal{A}_{Qq \rightarrow Qq}^{(2g)(8,-)(1)} - \Gamma_{qq}^{c(0)} \Gamma_{QQ}^{c(0)} \frac{s}{t} \omega^{(1)}(t) \left[\ln\left(\frac{s}{-t}\right) + \ln\left(\frac{-s}{-t}\right) \right] \right\}. \quad (3.12)$$

The value $\mathcal{A}_{Qq \rightarrow Qq}^{(2g)(8,-)(1)}$ is given by the contribution of two diagrams of Fig. 6 through the same procedure (3.1) for the lowest line of these diagrams to project on the negative signature and the colour octet in the t -channel. In this way one gets

$$\mathcal{A}_{Qq \rightarrow Qq}^{(2g)(8,-)(1)} = \frac{1}{4} N \langle 1' | t^c | 1 \rangle \langle B' | t^c | B \rangle (D_3 - D_3(s \leftrightarrow -s)), \quad (3.13)$$

where the D_3 is the amplitude represented by the diagram of Fig. 6(a) with omitted colour factors. The calculation of this diagram is quite simple and we do not present any details here. The result for $\delta^{(2g)}$ can be obtained in exact form without ϵ -expansion

$$\begin{aligned} \delta^{(2g)}(t) &= \frac{1}{2} \omega^{(1)}(t) \left[\frac{1}{\epsilon} + \psi(1) + \psi(1 - \epsilon) - 2\psi(1 + \epsilon) \right] \\ &\approx -g^2 N \frac{\Gamma(2 - \epsilon)}{(4\pi)^{2+\epsilon}} \frac{1}{\epsilon} (-t)^\epsilon \left(\frac{1}{\epsilon} + 1 + \epsilon - 4\epsilon\psi'(1) \right), \end{aligned} \quad (3.14)$$

where the last approximate equality shows the expanded in ϵ result which is enough for our purposes. Now, using Eqs. (2.7), (2.9), (3.2) - (3.5), (3.9), (3.11) and (3.14) we obtain

$$\Gamma_{\gamma^* q\bar{q}}^{(2g)c(1)} \left(e q_f g^3 N t_{i_1 i_2}^c \frac{\Gamma(2 - \epsilon)}{(4\pi)^{2+\epsilon}} \frac{1}{2\epsilon} \right)^{-1} = \left[\bar{u}_1 \left(2(-t)^\epsilon (2(1 + \epsilon) \ln x_2 - \epsilon\psi'(1)) \right) \frac{\hat{\Gamma}_1}{t_1} \right]$$

$$\begin{aligned}
& + \int_0^1 \frac{dy}{(-(1-y)t - yt_1)^{1-\epsilon}} 2(1+\epsilon)(t - 2y^\epsilon(t - t_1)) \frac{\hat{\Gamma}_1}{t_1} \\
& + \int_0^1 \int_0^1 \frac{dy_1 dy_2}{(-y_1 y_2 \kappa - t - y_2(t_1 - t) - y_1(t_2 - t))^{2-\epsilon}} \left\{ y_1^{\epsilon-1} (1 - y_1) y_2^{-\epsilon} \right. \\
& \quad \times \left(x_1^\epsilon x_2^{-\epsilon} - 2\epsilon^2 \psi'(1) \right) 2t \hat{\Gamma}_1 + (1 - y_1) 4t (ek_1) \\
& \quad \left. + \left(y_1^\epsilon y_2^{-\epsilon} x_1^\epsilon x_2^{-\epsilon} - 1 \right) 4x_2 t (ep_1) \right\} \frac{\not{p}_2}{s} v_2 \Big] - [1 \leftrightarrow 2]. \tag{3.15}
\end{aligned}$$

The last equality gives the integral representation for the one-loop two-gluon exchange part of the Reggeon-virtual photon effective vertex for the quark-antiquark production. Although all the integrals in (3.15) can be expressed in terms of elementary functions and dilogarithms with the necessary accuracy in ϵ -expansion, it seems more convenient to leave the result in such unintegrated form in order to have a possibility to use usual Feynman parametrization and to change orders of integrations over all Feynman parameters at subsequent calculation of the impact factor. Performing the integrations in Eq. (3.15) one loses this possibility and has to do a step back to an unintegrated result to restore it. Let us finally note, that the method of extraction of $\Gamma_{\gamma^* q \bar{q}}^{(2g)c(1)}$ from the corresponding part of the amplitude we used here is absolutely equivalent to one proposed in Ref. [13] and gives the same result that has been checked by direct comparison.

4 The one-loop correction: the one-gluon exchange diagrams

In this section we consider the contribution of the one-gluon exchange diagrams to the vertex $\Gamma_{\gamma^* q \bar{q}}^c$. It is presented by the diagrams of Fig. 7 with the gluon polarization vector equal to $-p_2^\mu/s$, as already was explained in the previous Section. Calculating the colour factors of the diagrams one can easily obtain the following representation

$$\Gamma_{\gamma^* q \bar{q}}^{(1g)c(1)} = N t_{i_1 i_2}^c \left\{ \left[-\frac{2C_F}{N} (R_1 + R_2) + \frac{N - 2C_F}{N} (R_3 + R_4) + R_5 + \tilde{R}_6 \right] - [1 \leftrightarrow 2] \right\}, \tag{4.1}$$

with the usual notation

$$C_F = \frac{N^2 - 1}{2N} \tag{4.2}$$

and the notations $2R_1, \dots, 2R_4, -2R_5$ and $4\tilde{R}_6$ for the amplitudes represented by the diagrams of Figs. 7(1), ... , (4), (5) and (6) respectively with omitted colour generators in any vertex and the external virtual gluon polarization vector equal to p_2^μ/s . While the definition of R_1, \dots, R_4 is absolutely clear, the R_5 and \tilde{R}_6 are not well defined by the above prescription because of presence of three-gluon vertices in the corresponding diagrams Figs. 7(5) and 7(6). To complete their definition we have indicated explicitly the momenta and vector indices for the three-gluon vertex for which the following expression should be used after the omission of colour generators

$$\gamma_{\lambda\nu\mu}(-k - q, k) = ig [-g_{\lambda\nu}(2k + q)_\mu + g_{\lambda\mu}(k + 2q)_\nu + g_{\nu\mu}(k - q)_\lambda]. \tag{4.3}$$

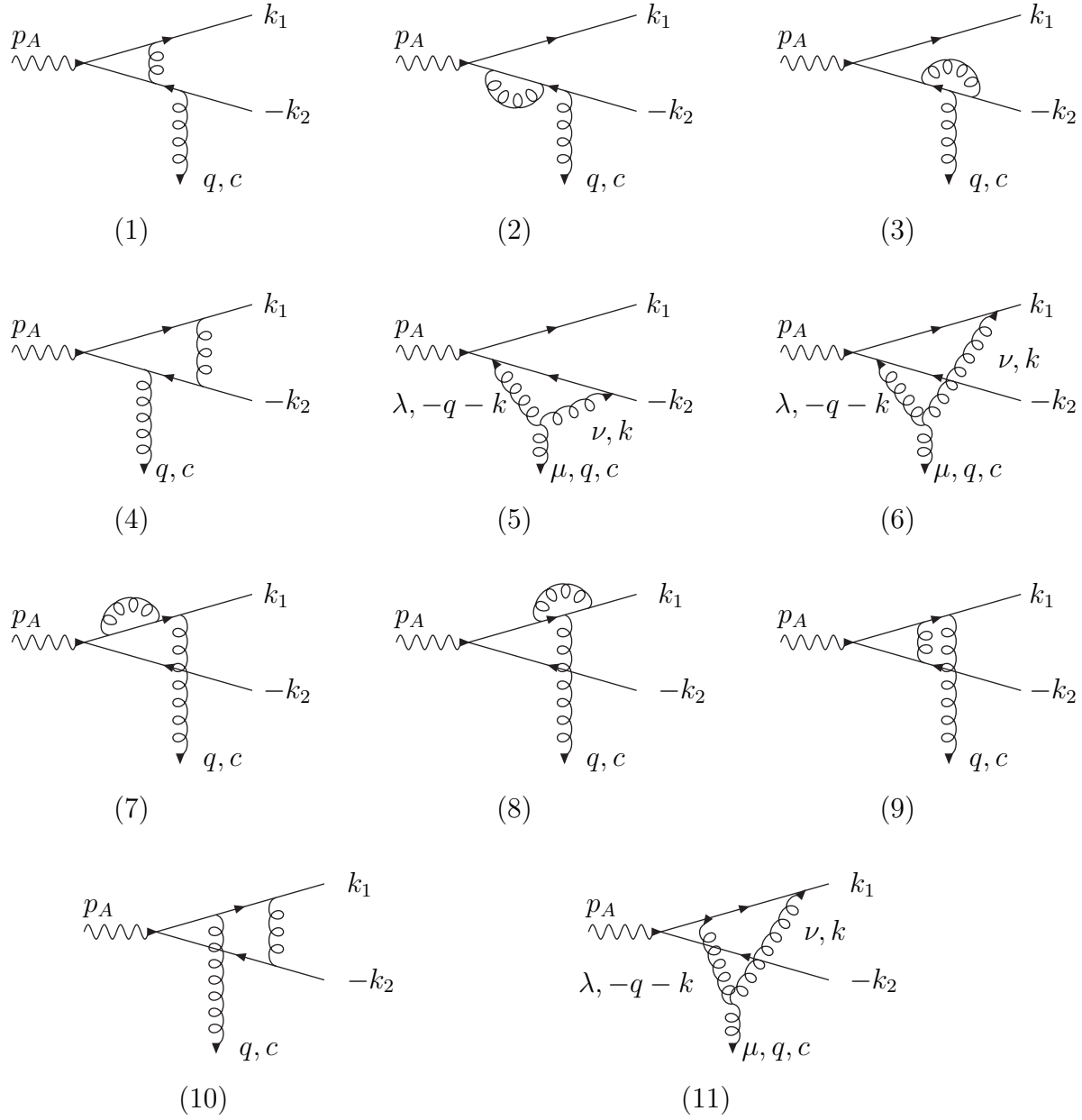


Figure 7: The diagrams corresponding to the correction $\Gamma_{\gamma^* q \bar{q}}^{(1g)c(1)}$.

The calculation of R_1, R_2, R_3 and R_5 is simple and we present here only the list of the results in integral form without any details

$$\begin{aligned}
R_1 = & -eq_f g^3 \frac{\Gamma(2-\epsilon)}{(4\pi)^{2+\epsilon}} \frac{1}{2\epsilon} \bar{u}_1 \int_0^1 \frac{dy}{((1-y)Q^2 - yt_1)^{1-\epsilon}} \left\{ (1+2\epsilon) \frac{Q^2}{t_1} \hat{\Gamma}_1 + 2\epsilon(ep_1) \right. \\
& \left. + y \left[(1-2\epsilon) \left(\frac{Q^2}{t_1} + 1 \right) \hat{\Gamma}_1 + 2(2-\epsilon)(ek_1) \right] \right\} \frac{\not{p}_2}{s} v_2, \quad (4.4)
\end{aligned}$$

$$R_2 = -eq_f g^3 \frac{\Gamma(2-\epsilon)}{(4\pi)^{2+\epsilon}} \frac{1}{2\epsilon} \bar{u}_1 \frac{\hat{\Gamma}_1}{(-t_1)^{1-\epsilon}} \frac{\not{p}_2}{s} v_2, \quad (4.5)$$

$$R_3 = eq_f g^3 \frac{\Gamma(2-\epsilon)}{(4\pi)^{2+\epsilon}} \frac{1}{2\epsilon} \bar{u}_1 \int_0^1 \frac{dy}{(-(1-y)t - yt_1)^{1-\epsilon}} \left\{ (1+2\epsilon) \frac{t}{t_1} \hat{\Gamma}_1 \right.$$

$$\begin{aligned}
& \left. \left(\vec{k}_2 \vec{q} - i\lambda P \right) \delta_{\lambda, \xi} \right] + (1-z)(y_1 x_1 + (1-y_2)x_2) \left[\left(x_1 (\vec{k}_2 \vec{q} - i\xi P) - z y_1 (\vec{k}_1 \vec{q} - i\xi P - x_1 t_1) \right) \right. \\
& \times \sqrt{2} q Q \delta_{\lambda, 0} + z(1-y_1-y_2) \left((\vec{k}_1^2 \vec{q}^2 - x_1 t_1 (\vec{k}_1 \vec{q} + i\lambda P)) (\delta_{\lambda, -\xi} - \delta_{\lambda, \xi}) + 2(\vec{k}_1 \vec{k}_2 - x_1 x_2 Q^2) \right. \\
& \quad \left. \left. \times (\vec{k}_1 \vec{q} + i\lambda P) \delta_{\lambda, -\xi} - (\vec{k}_1 \vec{q} - i\xi P - x_1 t_1) \sqrt{2} q Q x_2 \delta_{\lambda, 0} \right) \right. \\
& \quad \left. \left. + z y_2 \vec{q}^2 \left((\vec{k}_1 \vec{q} + i\lambda P - x_1 t_1) (\delta_{\lambda, -\xi} - \delta_{\lambda, \xi}) - 2(\vec{k}_1 \vec{k}_2 - x_1 x_2 Q^2) \delta_{\lambda, \xi} \right) \right] \right\} \quad (4.11)
\end{aligned}$$

and

$$\begin{aligned}
R_6^{(r)} &= \frac{e q_f g^3}{(4\pi)^2 \sqrt{2} x_1 x_2 \vec{q}^2} \int_0^1 \int_0^1 \frac{dy_1 dy_2}{(-y_1 y_2 \kappa - t - y_2(t_1 - t) - y_1(t_2 - t))^2} \\
& \times \left(y_1 \delta_{\lambda, 0} \sqrt{2} q Q x_1 \left\{ (x_1 x_2 Q^2 - \vec{k}_1 \vec{k}_2 - i\xi P) (1 - 3x_2) + 2x_2(t_2 - t) \right\} + (1 - y_1) \right. \\
& \quad \left. \times \left\{ 2(-y_1 y_2 \kappa - t - y_2(t_1 - t) - y_1(t_2 - t)) + y_1(t_2 - t - \kappa) \right\} x_1 x_2 \right. \\
& \quad \left. \times \left((\delta_{\lambda, -\xi} + \delta_{\lambda, \xi}) (\vec{k}_1 \vec{q} + i\lambda P) - \delta_{\lambda, 0} \sqrt{2} q Q x_1 \right) + \left[2x_1 t_1 + 2x_2 t_2 - 2t - y_2 x_2 (t_2 - t - \kappa) \right] \right. \\
& \quad \left. \times \left(\delta_{\lambda, 0} \sqrt{2} q Q x_1 x_2 - \delta_{\lambda, -\xi} x_2 (\vec{k}_1 \vec{q} + i\lambda P) - \delta_{\lambda, \xi} x_1 (\vec{k}_2 \vec{q} - i\lambda P) \right) \right. \\
& \quad \left. - \left[t(2x_1 \delta_{\lambda, \xi} + 3x_2 \delta_{\lambda, -\xi}) + y_1 x_1 (t \delta_{\lambda, -\xi} - \delta_{\lambda, 0} \sqrt{2} q Q x_1) \right] (x_1 x_2 Q^2 - \vec{k}_1 \vec{k}_2 - i\xi P) \right. \\
& \quad \left. + \left[3(x_2^2 t_2 \delta_{\lambda, -\xi} - x_1^2 t_1 \delta_{\lambda, \xi}) + y_1 x_1 x_2 (t_2 \delta_{\lambda, -\xi} - t_1 \delta_{\lambda, \xi}) - y_1 x_1 Q^2 \delta_{\lambda, \xi} \right] (\vec{k}_1 \vec{q} + i\lambda P) \right. \\
& \quad \left. + x_1 t \left[3x_2^2 Q^2 \delta_{\lambda, -\xi} - 3\vec{k}_1^2 \delta_{\lambda, \xi} + y_1 x_1 Q^2 (\delta_{\lambda, -\xi} x_2 + \delta_{\lambda, \xi} x_1) + 2y_2 x_2 \kappa \delta_{\lambda, \xi} \right] \right\}. \quad (4.12)
\end{aligned}$$

The result for the correction $\Gamma_{\gamma^* q \bar{q}}^{(1g)^{c(1)}}$ is obtained now by Eq. (4.1) with the replacement

$$\tilde{R}_6 \rightarrow R_6, \quad (4.13)$$

where R_1, R_2, R_3 and R_5 are presented by Eqs. (4.4), (4.5), (4.6) and (4.7) respectively and R_4 and R_6 are given by Eqs. (4.9) - (4.12) and by the relation

$$R_{4,6} = R_{4,6}^{(s)} + R_{4,6}^{(r)}. \quad (4.14)$$

5 The total one-loop correction

There is one more one-loop contribution to the vertex $\Gamma_{\gamma^* q \bar{q}}^c$ related to the t -channel gluon self-energy. It is given by the half of the amplitude schematically represented at Fig. 8 with the gluon polarization vector equal to $-p_2^\mu/s$, as was already explained in the Section 3. To find the correction $\Gamma_{\gamma^* q \bar{q}}^{(se)^{c(1)}}$ one should only know the one-loop gluon vacuum polarization and the Born Reggeon-virtual photon vertex. We obtain:

$$\Gamma_{\gamma^* q \bar{q}}^{(se)^{c(1)}} \left(e q_f g^3 N t_{i_1 i_2}^c \frac{\Gamma(2-\epsilon)}{(4\pi)^{2+\epsilon}} \frac{1}{2\epsilon} \right)^{-1}$$

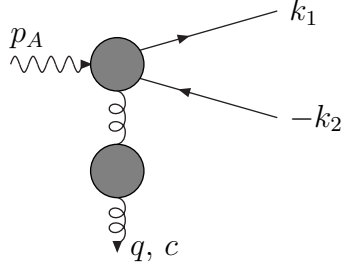


Figure 8: Schematic representation of the correction $\Gamma_{\gamma^* q\bar{q}}^{(se)c(1)}$.

$$= \left[\bar{u}_1 (-t)^\epsilon \left\{ \frac{5}{3} - \frac{2n_f}{3N} + \epsilon \left(\frac{4n_f}{9N} - \frac{16}{9} \right) \right\} \frac{\hat{\Gamma}_1}{t_1} \frac{\not{p}_2}{s} v_2 \right] - [1 \leftrightarrow 2], \quad (5.1)$$

where n_f is the number of quark flavours.

We present the total one-loop correction to the vertex of the quark-antiquark production in the virtual photon-Reggeized gluon collision in the form:

$$\Gamma_{\gamma^* q\bar{q}}^{c(1)} = \Gamma_{\gamma^* q\bar{q}}^{(sing)c(1)} + \Gamma_{\gamma^* q\bar{q}}^{(reg)c(1)}, \quad (5.2)$$

with

$$\Gamma_{\gamma^* q\bar{q}}^{(reg)c(1)} = N t_{i_1 i_2}^c \left\{ \left[\frac{N - 2C_F}{N} R_4^{(r)} + R_6^{(r)} \right] - [1 \leftrightarrow 2] \right\} \quad (5.3)$$

where $R_4^{(r)}$ and $R_6^{(r)}$ are given by Eqs. (4.11) and (4.12) correspondingly, and

$$\begin{aligned} \Gamma_{\gamma^* q\bar{q}}^{(sing)c(1)} &= \Gamma_{\gamma^* q\bar{q}}^{(2g)c(1)} + \Gamma_{\gamma^* q\bar{q}}^{(se)c(1)} \\ &+ N t_{i_1 i_2}^c \left\{ \left[-\frac{2C_F}{N} (R_1 + R_2) + \frac{N - 2C_F}{N} (R_3 + R_4^{(s)}) + R_5 + R_6^{(s)} \right] - [1 \leftrightarrow 2] \right\} \end{aligned} \quad (5.4)$$

where $\Gamma_{\gamma^* q\bar{q}}^{(2g)c(1)}$, $\Gamma_{\gamma^* q\bar{q}}^{(se)c(1)}$, $R_1 - R_3$, R_5 , $R_4^{(s)}$ and $R_6^{(s)}$ are defined in Eqs. (3.15), (5.1), (4.4) - (4.6), (4.7), (4.9) and (4.10) respectively. Using the last set of relations one can easily obtain

$$\begin{aligned} \Gamma_{\gamma^* q\bar{q}}^{(sing)c(1)} &\left(e q_f g^3 N t_{i_1 i_2}^c \frac{\Gamma(2-\epsilon)}{(4\pi)^{2+\epsilon}} \frac{1}{2\epsilon} \right)^{-1} = \left[\bar{u}_1 \left((-t)^\epsilon \left\{ \frac{5}{3} - \frac{2n_f}{3N} + 4(1+\epsilon) \ln x_2 + 2\epsilon \left(\frac{2n_f}{9N} \right. \right. \right. \right. \\ &- \frac{8}{9} - \psi'(1) \left. \left. \left. \right\} \frac{\hat{\Gamma}_1}{t_1} + \frac{2C_F}{N} \frac{\hat{\Gamma}_1}{(-t_1)^{1-\epsilon}} + \frac{2C_F}{N} \int_0^1 \frac{dy}{((1-y)Q^2 - yt_1)^{1-\epsilon}} \left\{ (1+2\epsilon) \frac{Q^2}{t_1} \hat{\Gamma}_1 + 2\epsilon(e p_1) \right. \right. \right. \\ &+ y \left[(1-2\epsilon) \left(\frac{Q^2}{t_1} + 1 \right) \hat{\Gamma}_1 + 2(2-\epsilon)(ek_1) \right] \left. \left. \left. \right\} + \frac{1}{N} \int_0^1 \frac{dy}{(-(1-y)t - yt_1)^{1-\epsilon}} \right. \right. \\ &\times \left\{ 2 \left((1+3\epsilon)N - (1+2\epsilon)C_F \right) \frac{t}{t_1} \hat{\Gamma}_1 - (2+\epsilon)N \hat{\Gamma}_1 + (1+2\epsilon)N x_2 \left(\hat{\Gamma}_1 + \hat{\Gamma}_2 - 2(e_\perp q_\perp) \right) \right. \\ &- y^\epsilon 4(1+\epsilon)N \left(\frac{t}{t_1} - 1 \right) \hat{\Gamma}_1 + y \left[2 \left((1-\epsilon)N - (1-2\epsilon)C_F \right) \left(\frac{t}{t_1} - 1 \right) \hat{\Gamma}_1 + \left((1-2\epsilon)N \right. \right. \\ &\left. \left. \left. - 2(2-\epsilon)C_F \right) x_2 \left(\hat{\Gamma}_1 + \hat{\Gamma}_2 - 2(e_\perp q_\perp) \right) \right] \left. \left. \right\} + \frac{N - 2C_F}{N} \times \right. \end{aligned}$$

$$\begin{aligned}
& \int_0^1 \int_0^1 \int_0^1 \frac{dz dy_1 dy_2 \theta(1-y_1-y_2) z^{1+\epsilon} 2\epsilon\kappa}{[zy_1y_2(-\kappa-i\delta) + (1-z)(y_1Q^2 - y_2t - (1-y_1-y_2)t_1)]^{2-\epsilon}} [(1-y_1-y_2) \times \\
& \quad \left((1-z(1-y_2)) x_2 (\hat{\Gamma}_1 + \hat{\Gamma}_2 - 2(e_\perp q_\perp)) - \hat{\Gamma}_1 \right) - 2y_1(1-zy_1)(ek_1)] \\
& \quad + \int_0^1 \int_0^1 \frac{dy_1 dy_2}{(-y_1y_2\kappa - t - y_2(t_1-t) - y_1(t_2-t))^{2-\epsilon}} \left\{ y_1^{\epsilon-1}(1-y_1)y_2^{-\epsilon} \right. \\
& \quad \times \left(x_1^\epsilon x_2^{-\epsilon} - 2\epsilon^2 \psi'(1) \right) 2t\hat{\Gamma}_1 + \left(y_1^\epsilon y_2^{-\epsilon} x_1^\epsilon x_2^{-\epsilon} - 1 \right) 4x_2 t(ep_1) + (1-y_1) \left[2(t_2-t)\hat{\Gamma}_1 \right. \\
& \quad \left. \left. - x_1 t_1 (\hat{\Gamma}_1 + \hat{\Gamma}_2 - 2(e_\perp q_\perp)) + 4t(ek_1) \right] + y_1(1-y_1) \left[4(t_2-t)(ek_1) \right. \right. \\
& \quad \left. \left. + x_1(t_1+Q^2) (\hat{\Gamma}_1 + \hat{\Gamma}_2 - 2(e_\perp q_\perp)) \right] \right\} \frac{\not{p}_2}{s} v_2 \Big] - [1 \leftrightarrow 2]. \tag{5.5}
\end{aligned}$$

The relations (5.2), (5.3), (5.5) together with Eqs. (4.11, 4.12) present the one-loop correction to the $\gamma^* R \rightarrow q\bar{q}$ vertex.

6 Discussion

In this paper we have calculated the effective vertices for the Reggeon-virtual photon interaction. Starting from already known expressions (2.9), (2.10) for the $q\bar{q}$ production vertex in the Born approximation we have represented this vertex in the helicity basis (2.16) and then have obtained in the same approximation the vertex (2.19) for the $q\bar{q}g$ production. The most of the paper is devoted to the calculation of the one-loop corrections for the $q\bar{q}$ production vertex, which are presented in Eqs. (5.2), (5.5), (5.3), (4.11) and (4.12). In order to simplify the presentation the last three results are given in the helicity basis, that caused the representation in this basis also the Born $q\bar{q}$ production vertex (2.16).

The obtained results can be used for theoretical analysis of a number of processes related to the quark-antiquark production in the photon fragmentation region. In particular, they are necessary for calculation of the virtual photon impact factor at the next-to-leading order (see Eq. (1.3)). We have used the integral representation for a part of the one-loop corrections to the $q\bar{q}$ production vertex since it is convenient for further calculation of the virtual photon impact factor in the next-to-leading order.

Note, that everywhere in the paper g is the unrenormalized coupling constant, so that the one-loop correction contains the ultraviolet singularities in ϵ . In order to remove them one should only express g in terms of the renormalized coupling constant $g(\mu)$. After the renormalization there still remain the infrared singularities, which must cancel in physical quantities (in the virtual photon impact factor they cancel [13] with corresponding terms in the contributions from the additional gluon emission and from the counterterm (see Eq. (1.3)).

Acknowledgment: Two of us (M.K. and D.I.) thank the Dipartimento di Fisica della Università della Calabria for the warm hospitality while part of this work was done. D.I. was supported by Alexander von Humboldt Stiftung.

A Appendix A

In this section we explain very briefly important steps for calculation of the most complicated diagram D_2 (Fig. 5(2)) to make our results checkable step by step. According to its definition we obtain from the corresponding diagram

$$D_2 = \frac{-ieq_f g^4}{2(2\pi)^D} \times \int \frac{d^D k \bar{u}_1 \gamma^\mu (\not{k} + \not{p}_A - \not{k}_2) \not{\epsilon} (\not{k} - \not{k}_2) \gamma^\lambda v_2 \bar{u}_{B'} \gamma^\rho (\not{k} + \not{p}_{B'}) \gamma^\nu u_B g_{\mu\nu} g_{\lambda\rho}}{[(k + p_{B'})^2 + i\delta][(k + p_A - k_2)^2 + i\delta][(k - k_2)^2 + i\delta][k^2 + i\delta][(k + q)^2 + i\delta]} . \quad (\text{A.1})$$

It was explained in details in Ref. [13], that the negative t -channel signature combination of the two pentagon diagrams of Fig. 5, or, that is the same, the $s \leftrightarrow -s$ antisymmetric part of the D_2 , gets the contribution only from the integration region where

$$\vec{q}^2 \sim \vec{k}^2 \sim |kp_1| \ll |kp_2| \sim s , \quad (\text{A.2})$$

and therefore we can replace from the beginning

$$\frac{1}{(k + p_{B'})^2 + i\delta} \rightarrow P \frac{1}{2kp_2} \quad (\text{A.3})$$

and understand this singularity in a sense of the principal value everywhere below. In order to simplify also the numerator of the D_2 we use the familiar replacement (2.3) for the t -channel gluon propagators. These simplifications lead to the following representation for D_2

$$D_2 = -2ieq_f g^4 s \bar{u}_{B'} \frac{\not{p}_1}{s} u_B \int \frac{d^D k}{(2\pi)^D} \times \frac{1}{[(k + p_A - k_2)^2 + i\delta][(k - k_2)^2 + i\delta][k^2 + i\delta][(k + q)^2 + i\delta]} \times \bar{u}_1 \left\{ \not{\epsilon} (\not{k} - \not{k}_2) + (\not{k} + \not{q}) \not{\epsilon} + \frac{s}{2kp_2} (x_1 \not{\epsilon} (\not{k} - \not{k}_2) - x_2 (\not{k} + \not{q}) \not{\epsilon}) \right\} \frac{\not{p}_2}{s} v_2 . \quad (\text{A.4})$$

Since the structure of D_2 is like the box diagram with two massive external lines in opposite corners, it is convenient to perform the Feynman parametrization joining first the pairs of propagators which meet in each of the vertices with massless external lines, and then to join two denominators obtained in this way using the third Feynman parameter. Doing so we naturally get the result of momentum integration in the form where the dependence on the third Feynman parameter factorizes and the integration over this parameter can be performed straightforwardly. So we use in Eq. (A.4) the representation

$$\frac{1}{[(k + p_A - k_2)^2 + i\delta][(k - k_2)^2 + i\delta][k^2 + i\delta][(k + q)^2 + i\delta]} = 6 \int_0^1 \frac{d^3 y y_3 (1 - y_3)}{[k^2 + 2k((1 - y_3)(q + y_1 k_1) - y_3 y_2 k_2) + (1 - y_3)((1 - y_1)t + y_1 t_2) + i\delta]^4} . \quad (\text{A.5})$$

For the term with $1/(2kp_2)$ in Eq. (A.4) we use the relation

$$\frac{1}{a^4 b} = 4 \int_0^\infty \frac{du}{(a + bu)^5}, \quad (\text{A.6})$$

which leads, together with Eq. (A.5), to the expression

$$D_2 = -12ieq_f g^4 s \bar{u}_{B'} \frac{\not{p}_1}{s} u_B \bar{u}_1 \int_0^1 d^3 y y_3 (1 - y_3) \int \frac{d^D k}{(2\pi)^D} \left\{ \frac{\not{\epsilon} (k - k_2) + (k + \not{q}) \not{\epsilon}}{[(k + p)^2 - y_3(1 - y_3)b^2 + i\delta]^4} \right. \\ \left. + 4 \int_0^\infty du \frac{s(x_1 \not{\epsilon} (k - k_2) - x_2 (k + \not{q}) \not{\epsilon})}{[(k + p + up_2)^2 - y_3(1 - y_3)b^2 - su((1 - y_3)y_1 x_1 - y_2 y_3 x_2) + i\delta]^5} \right\} \frac{\not{p}_2}{s} v_2, \quad (\text{A.7})$$

where the notations

$$p = (1 - y_3)(q + y_1 k_1) - y_2 y_3 k_2, \quad b^2 = (1 - y_2)(-(1 - y_1)t - y_1 t_2) + y_2(-(1 - y_1)t_1 + y_1 Q^2) \quad (\text{A.8})$$

have been introduced.

Now the k -integration and then the integration over u are immediate to perform. The result is:

$$D_2 = g \bar{u}_{B'} \frac{\not{p}_1}{s} u_B \frac{2s}{t} eq_f g^3 \frac{\Gamma(2 - \epsilon)}{(4\pi)^{2+\epsilon}} t \bar{u}_1 \int_0^1 \frac{d^2 y}{(b^2)^{2-\epsilon}} P \int_0^1 \frac{dy_3}{[y_3(1 - y_3)]^{1-\epsilon}} \times \\ \left\{ (\not{q} - \not{p}) \not{\epsilon} - \not{\epsilon} (k_2 + \not{p}) + \frac{x_2 (\not{q} - \not{p}) \not{\epsilon} + x_1 \not{\epsilon} (k_2 + \not{p})}{x_1((1 - y_3)y_1 - zy_3 y_2)} \right\} \frac{\not{p}_2}{s} v_2, \quad (\text{A.9})$$

with

$$z = \frac{x_2}{x_1}. \quad (\text{A.10})$$

After some simplifying algebra with the use of the fact that D_2 enters into our result for the vertex only in the antisymmetric under the replacement $1 \leftrightarrow 2$ combination (see Eq. (3.2)) we come to the representation

$$D_2 = 2g \bar{u}_{B'} \frac{\not{p}_1}{s} u_B \frac{2s}{t} eq_f g^3 \frac{\Gamma(2 - \epsilon)}{(4\pi)^{2+\epsilon}} \\ \times \bar{u}_1 t \frac{\not{p}_2}{s} \int_0^1 \int_0^1 \frac{dy_1 dy_2}{[(1 - y_2)(-(1 - y_1)t - y_1 t_2) + y_2(-(1 - y_1)t_1 + y_1 Q^2)]^{2-\epsilon}} \left[\frac{1 - y_1}{x_1} \right. \\ \times (2x_2(k_{1\perp} e_\perp) - \not{\epsilon}_\perp k_{1\perp}) P \int_0^1 \frac{dy_3 y_3^{\epsilon-1} (1 - y_3)^\epsilon}{((1 - y_3)y_1 - zy_3 y_2)} + x_2(ep_1) \\ \left. \times P \int_0^1 \frac{dy_3 y_3^{\epsilon-1} (1 - y_3)^{\epsilon-1}}{((1 - y_3)y_1 - zy_3 y_2)} + \frac{2}{\epsilon} ((ek_1)(1 - y_1) - x_2(ep_1)) \right] v_2, \quad (\text{A.11})$$

and, finally, the relations

$$P \int_0^1 \frac{dy_3 y_3^{\epsilon-1} (1 - y_3)^\epsilon}{((1 - y_3)y_1 - zy_3 y_2)} = \frac{1}{\epsilon} \left(1 - 2\epsilon^2 \psi'(1) \right) z^{-\epsilon} y_1^{\epsilon-1} y_2^{-\epsilon} \quad (\text{A.12})$$

and

$$P \int_0^1 \frac{dy_3 y_3^{\epsilon-1} (1 - y_3)^{\epsilon-1}}{((1 - y_3)y_1 - zy_3 y_2)} = \frac{1}{\epsilon} \left(1 - 2\epsilon^2 \psi'(1) \right) z^{-\epsilon} \left(y_1^{\epsilon-1} y_2^{-\epsilon} - z^{2\epsilon-1} y_2^{\epsilon-1} y_1^{-\epsilon} \right), \quad (\text{A.13})$$

which are valid with an enough for us accuracy in the ϵ -expansion, lead to the result (3.5).

References

- [1] V.S. Fadin, E.A. Kuraev, L.N. Lipatov, Phys. Lett. **B60** (1975) 50; E.A. Kuraev, L.N. Lipatov and V.S. Fadin, Zh. Eksp. Teor. Fiz. **71** (1976) 840 [Sov. Phys. JETP **44** (1976) 443]; **72** (1977) 377 [**45** (1977) 199]; Ya.Ya. Balitskii and L.N. Lipatov, Sov. J. Nucl. Phys. **28** (1978) 822.
- [2] A.M. Cooper-Sarkar, R.C.E. Devenish and A. De Roeck, Int. J. Mod. Phys. **A13** (1998) 3385, and references therein.
- [3] L.N. Lipatov, V.S. Fadin, Sov. J. Nucl. Phys. **50** (1989) 712.
- [4] V.S. Fadin, R. Fiore, M.I. Kotsky, Phys. Lett. **B359** (1995) 181.
- [5] V.S. Fadin, R. Fiore, M.I. Kotsky, Phys. Lett. **B387** (1996) 593.
- [6] V.S. Fadin, L.N. Lipatov, Nucl. Phys. **B406** (1993) 259.
- [7] V.S. Fadin, R. Fiore, A. Quartarolo, Phys. Rev. **D50** (1994) 5893; V.S. Fadin, R. Fiore, M.I. Kotsky, Phys. Lett. **B389** (1996) 737; V.S. Fadin, L.N. Lipatov, Nucl. Phys. **B477** (1996) 767; V.S. Fadin, M.I. Kotsky, L.N. Lipatov, Phys. Lett. **B415** (1997) 97; V.S. Fadin, R. Fiore, A. Flachi, M.I. Kotsky, Phys. Lett. **B422** (1998) 287.
- [8] S. Catani, M. Ciafaloni, F. Hautman, Phys. Lett. **B242** (1990) 97; Nucl. Phys. **B366** (1991) 135; G. Camici and M. Ciafaloni, Phys. Lett. **B386** (1996) 341; Nucl. Phys. **B496** (1997) 305.
- [9] V.S. Fadin, L.N. Lipatov, Phys. Lett. **B429** (1998) 127.
- [10] G. Camici and M. Ciafaloni, Phys. Lett. **B430** (1998) 349.
- [11] V.S. Fadin, R. Fiore, Phys. Lett. **B440** (1998) 359.
- [12] V.S. Fadin, R. Fiore, M.I. Kotsky and A. Papa, Phys. Rev. **D61** (2000) 094006; Phys. Rev. **D61** (2000) 094005.
- [13] V.S. Fadin and A.D. Martin, Phys. Rev. **D60** (1999) 114008.
- [14] V. Fadin, D. Ivanov, M. Kotsky, In: New Trends in High-Energy Physics, Ed. L.L. Jenkovszky, Kiev, 2000, pp. 190-194; hep-ph/0007119.